J. Biochem. 119, 1024-1032 (1996)

Innocuous Labeling of the Subfragment-2 Region of Skeletal Muscle Heavy Meromyosin with a Fluorescent Polyacrylamide Nanobead and Visualization of Individual Heavy Meromyosin Molecules[1]

Yuki Kunioka and Toshio Ando[2]

Department of Physics, Faculty of Science, Kanazawa University, Kanazawa, Ishikawa 920-11

Received for publication, October 19, 1995

We have studied transglutaminase-catalyzed incorporation of monodansylcadaverine and monobiotincadaverine into rabbit skeletal muscle heavy meromyosin (HMM). The incorporation of dansylcadaverine reached saturation at 4 mol per 1 mol of HMM. An electrophoretogram of the chymotryptic digest of the dansyl-labeled HMM revealed that the labeling took place primarily in the S-2 region of HMM. Atomic force microscopic images and electron micrographs of the complexes of the biotinylated HMM and UltraAvidin-coated fluorescent polyacrylamide nanoparticles revealed that the biotinylated site on S-2 was very close to the C-terminus (near the S-2/light meromyosin junction). In keeping with this result, together with HMM's key sites being localized on the S-1 region, the enzymatic conjugation of biotincadaverine had no influence upon the actin-activated ATPase activity of HMM or upon the ability of HMM to actuate sliding of actin filaments in *in vitro* motility assay. Attachment of an UltraAvidin-coated fluorescent nanobead to the biotinylated HMM also did not alter the motile activity of HMM. Thus, we can optically pinpoint individual HMM molecules in a sample, which will facilitate handling and manipulation of single HMM molecules and observation of their functional behavior.

Key words: actin, avidin, biotin, fluorescent nanobead, myosin.

Sheetz and Spudich in 1983 (*1*) and Shimmen and Yano in 1984 (*2*) independently developed a technique to observe movement of myosin-coated latex beads on actin cables *in vitro*. In 1984 Yanagida *et al.* demonstrated that single actin filaments labeled with fluorescent phalloidin could be visualized under a fluorescence microscope (*3*). These studies were soon followed by others that made it possible to observe sliding movement (*4*) and force generation (*5*) of single actin filaments interacting with myosin fixed onto a flat substratum. Since then, with the help of new technology such as laser optical trapping (*6*), several types of *in vitro* sliding and force assay systems, not only for actomyosin but also for other motor proteins, have been developed (*e.g.*, Refs. *7-10*). The size of the system that can be observed has been greatly reduced from whole muscle to muscle fibers, myofibrils, single actin, and myosin filaments, and finally to latex beads coated with a small number of myosin molecules. The next stage seems to be "uni-molecular physiology," in which, with the aid of new technology such as scanning probe microscopy (see reviews, Refs. *11* and *12*), we would be able to observe the morphological, mechanical, and enzymatic behavior of individual motor protein molecules. To achieve this, we first need to pinpoint individual motor proteins in a sample. This can be done with fluorescence microscopy, if each motor protein can be linked, without losing its motile activity, to a bright fluorophore or to a small fluorescent bead. Chemical labeling of myosin has been extensively carried out, with the main targets for labeling being heavy chains [Cys-697 (*13*), Cys-707 (*14*), Lys-83 (*15*), *etc.*] and regulatory light chains (LC2) (Cys-157, Cys-128) (*16-18*), all of which reside on myosin heads. The labeling of myosin head heavy chains alters the ATPase properties (*19*) and often abolishes the motile activity (*20*). Although LC2-labeled myosin can retain its motile function (*18, 21*), the labeling procedure requires several steps (*22*) and the attachment to LC2 of a fluorescent bead whose size is comparable to that of a myosin head is likely to interfere with actin-myosin interaction. Since the S-2 region of myosin does not seem to be involved in myosin's motile function (*23*), the S-2 region should be a preferred target to be labeled with a fluorophore or a fluorescent bead. No one, however, has yet succeeded in selective labeling of the S-2 region by chemical modification. Transglutaminases catalyze modification of proteins through the exchange of primary amines for ammonia at the γ-carboxamide group of glutamine residues (see review, Ref. *24*). This reaction, therefore, gives a potential method for the selective incorporation of functional groups into proteins under mild conditions. In 1985 Takashi carried out enzymatic labeling of actin, using guinea-pig

[1] This work was supported by a Grant-in-Aid for Science Research from the Ministry of Education, Science, Sports and Culture of Japan, and grants from Sumitomo Foundation and the Multi-disciplinary Science Foundation to T. Ando.

[2] To whom correspondence should be addressed. e-mail: tando @kenroku.ipc.kanazawa-u.ac.jp

Abbreviations: AOT, di-iso-octyl sodium sulfosuccinate; biotin-$(AC_5)_2$-sulfo-OSu, sulfosuccinimidyl *N*-[*N'*-(D-biotinyl)-6-aminohexanoyl]-6'-aminohexanoate; HABA, 2(4'-hydroxybenzeneazo)benzoic acid; HMM, heavy meromyosin; LC, light chain; PMSF, phenylmethylsulfonyl fluoride; S-1, subfragment-1; S-2, subfragment-2; TNBS, 2,4,6-trinitrobenzenesulfonic acid; TES, *N*-tris[hydroxymethyl]-methyl-2-aminoethanesulfonic acid.

liver transglutaminase and primary amine-containing fluorophores, to find a novel site for fluorophore conjugation (*25, 26*). Then Takashi, Giordano, and one of the authors (TA) carried out the enzymatic labeling of HMM and S-1 as well, and observed that HMM was labeled but S-1 was scarcely labeled with rhodaminecadaverine (*27*). This observation suggested that the S-2 region of HMM was predominantly labeled. In the present study, using different cadaverine derivatives, we have confirmed that this inference is correct, we have further identified the labeled site on S-2 as being near the C-terminus, and have examined the effects of the labeling on the HMM ATPase activity and the ability of HMM to glide actin filaments in an *in vitro* motility assay. By attaching an UltraAvidin-coated fluorescent nanobead to the enzymatically biotinylated HMM we have optically visualized individual HMM molecules that are bound to actin filaments at a low molar ratio of HMM to actin. Since the bead-attached HMM retains the motile activity to the same extent as non-modified HMM, its use should facilitate unimolecular physiological studies of the actomyosin motor system.

MATERIALS AND METHODS

Chemicals—Lyophilized guinea-pig liver transglutaminase and phenylmethylsulfonyl fluoride (PMSF) were purchased from Sigma. Egg white avidin was from Calzyme Laboratories. UltraAvidin was from Leinco Technologies. ATP, di-iso-octyl sodium sulfosuccinate (AOT), potassium persulfate, toluene, 2,4,6-trinitrobenzenesulfonic acid (TNBS), and chymotrypsin were from Wako Pure Chemical. Dansylcadaverine, biotincadaverine, biotin, succinimidyl tetramethylrhodamine, and succinimidyl rhodamine green were obtained from Molecular Probes. Tetramethylrhodamine-phalloidin was synthesized from amino phalloidin and succinimidyl tetramethylrhodamine as described previously (*28*). 2-(4′-Hydroxybenzeneazo)benzoic acid (HABA) was from Nacalai Tesque. Sulfosuccinimidyl *N*-[*N*′-(D-biotinyl)-6-amino hexanoyl]-6′-aminohexanoate [Biotin-$(AC_5)_2$-sulfo-OSu] was purchased from Dojindo Chemical. SDS and acrylamide (Wako Pure Chemical) were of electrophoretic grade. When acrylamide was used for the preparation of polyacrylamide nanobeads, it was re-crystallized twice in chloroform. All other chemicals were of analytical grade.

Protein Preparation—Myosin was prepared from rabbit back and leg skeletal muscles (*29*) and stored in 0.3 M KCl, 50% (v/v) glycerol at −20°C. HMM was obtained by chymotryptic digestion of myosin (*30*), purified by DEAE HPLC, and stored at −20°C in lyophilized form. The lyophilization was carried out in 0.12 M sucrose, 20 mM ammonium acetate, and 1 mM 2-mercaptoethanol. HMM used in the *in vitro* motility assay was obtained by chymotryptic digestion of freshly prepared (not glycerinated) myosin. After centrifugal removal of the non-digested myosin and light meromyosin in a solution of low ionic strength, HMM was quickly frozen in liquid nitrogen and stored in liquid nitrogen. Acetone powder of rabbit skeletal muscle was prepared as described (*31*). Actin was purified by the method of Spudich and Watt (*32*). The molar concentration of HMM was estimated on the basis of $E^{1\%}_{280}=7.5$ and a molecular weight of 3.5×10^5, with correction for the turbidity (1.93× the 330 nm absorbance was subtracted from the 280 nm absorbance). The molar concentration of F-actin was estimated on the basis of $E^{1\%}_{290}=6.7$ and a molecular weight of 4.2×10^4 (1.68× the 330 nm absorbance was subtracted from the 290 nm absorbance to correct for turbidity artifacts). For dansylcadaverine-incorporated HMM the protein concentration was determined by the method of Lowry *et al.* (*33*).

Enzymatic Labeling of HMM—Lyophilized guinea-pig transglutaminase (2 units) was dissolved in 1 ml of a solution containing 2 mM dithiothreitol plus buffer A (50 mM KCl, 20 μM PMSF, 1 mM 2-mercaptoethanol, 50 mM TES-KOH, pH 7.0). The solution was evenly divided into ten vials, which were then stored in liquid nitrogen. Before use, one vial of transglutaminase was thawed at 35°C, mixed with 320 μl of 50 mM dithiothreitol plus buffer A, and then incubated overnight at 4°C. HMM was dialyzed overnight against buffer A. Biotincadaverine (or dansylcadaverine) and HMM were mixed in buffer A plus 2 mM $CaCl_2$ to make final concentrations of 1 mM and 10 μM, respectively, and the mixture was incubated at 25°C. The reaction was started by the addition of transglutaminase (final, 0.025 unit/ml) to the mixture. To follow the time course of incorporation of biotincadaverine into HMM, aliquots of the reaction mixture were withdrawn at various times, made up to 3 mM EGTA to terminate the transglutaminase reaction, immediately cooled by introducing them into centrifuge tubes pre-cooled in ice water and centrifuged for 15 min at 230,000× *g*. The centrifugation was done as a pre-treatment for HPLC. For separation of HMM from transglutaminase and unreacted biotincadaverine the supernatants were then applied to an HPLC gel filtration column (Tosoh G3000SW_{XL}) equilibrated with buffer B (50 mM KCl, 1 mM EDTA, 20 μM PMSF, 1 mM 2-mercaptoethanol, 20 mM TES-KOH, pH 7.0). Enzymatically labeled HMM used for *in vitro* motility assay was obtained as follows. The transglutaminase reaction was allowed to continue for 3 h and terminated by the addition of 3 mM EGTA. Since HPLC gel filtration often reduces the motile activity of HMM, free biotincadaverine was removed by exhaustive dialysis against buffer B at 0°C. Transglutaminase was, however, not removed. The biotinylated HMM was frozen in liquid nitrogen and stored in liquid nitrogen.

Dansyl Assay—The concentration of dansylcadaverine conjugated to HMM was determined by measuring the fluorescence intensity at 550 nm with excitation at 330 nm. The fluorescence intensity of dansylcadaverine increased upon incorporation into HMM. Therefore, the dansyl-labeled HMM was digested exhaustively with a 50- to 100-fold molar excess of chymotrypsin for 12 h at room temperature, and then its fluorescence was measured. The fluorescence intensity was compared with that of a known concentration of free dansylcadaverine. The fluorescence spectrophotometer used was F-3010 (Hitachi).

Biotin Assay—The quantity of biotin incorporated into HMM was determined by titration with avidin in the presence of a given concentration of HABA. HABA binds to avidin at the biotin sites with much weaker affinity than biotin, concomitantly resulting in enhancement of its absorbance at around 510 nm (*34*). Since avidin might not be able to reach all the biotins conjugated to HMM, HMM that had been digested exhaustively with chymotrypsin was also assayed. Biotinylated HMM and its chymotryptic

digests were diluted in 200 mM KCl, 20 mM TES-KOH (pH 7.0), and 150 μM HABA. Then a small volume of avidin solution was added several times. The absorbance at 510 nm was read 10 min after each addition of avidin. The avidin binding to biotin was pre-determined in the same way as above, the biotinylated proteins being replaced with a known concentration of biotin. The spectrophotometer used was UV-260 (Shimadzu).

Preparation of Biotinylated Fluorescent Polyacrylamide Nanobeads—We had tried to use several types of commercially available fluorescent polystyrene nanobeads as tags for HMM. All of them, however, showed non-specific binding to HMM and to actin. We therefore decided to prepare nanobeads of polyacrylamide. Polyacrylamide nanoparticles were prepared by polymerization of acrylamide in an inverse microemulsion system stabilized by AOT emulsifier according to the method of Candau and Leong (*35*) with slight modifications. AOT was purified by filtering the methanolic solution through a polyethersulfone membrane (pore size 0.2 μm, Advantec, Tokyo) and dried under high vacuum at 60°C (*36*). For further drying it was heated at 80°C for 5 h at atmospheric pressure. The dried AOT (7.7 g) was dissolved in toluene (27.9 g). Acrylamide solution (acrylamide, 2.9 g; bis-acrylamide, 29 mg; water, 3.3 g) was added to the emulsifier solution under stirring. Nitrogen was bubbled at room temperature through the microemulsion for 30 min to eliminate oxygen. The microemulsion was incubated for 10 min at 45°C and polymerization was then initiated by the addition of potassium persulfate (5.55 mg dissolved in 0.15 ml of water). The W/O emulsion was gently stirred for 20 h at 45°C and then evaporated at 50°C under reduced pressure to remove toluene until the solution became slightly opaque. To precipitate the polyacrylamide particles, 40 ml of methanol was added. After exhaustive washing by several cycles of dispersion in methanol and sedimentation, the precipitate was dissolved in 20 ml of water. The solution was clarified by centrifugation at 15,000 $\times g$ for 30 min, and then lyophilized. An aliquot (20 mg) of the lyophilized powder was dissolved in 40 ml of anhydrous ethylenediamine. The powder did not dissolve well at room temperature, but heating to 70°C gave a transparent solution. The solution was incubated at 70°C for 3 h with vigorous stirring, and then cooled in ice-cold water. To precipitate the aminated polyacrylamide particles 20 ml of butanol was added (methanol would not work as a precipitant in ethylenediamine). The precipitate was exhaustively washed with methanol, then dissolved in 4 ml of water and this solution was dialyzed against water. The amount of free amino groups introduced into polyacrylamide beads was estimated by measuring the optical density at 425 nm after reaction with 2 mM TNBS for 1 h in 50 mM borate buffer (pH 9.0) and by using $\varepsilon_{425nm} = 5 \times 10^3\ M^{-1}$. The molar concentration of the aminated polyacrylamide beads was estimated by measuring the dry weight and using the molecular weight of 1×10^6 (see below). One particle contained about 200 amino groups. Biotinylation of the polyacrylamide beads was carried out as follows. Biotin-$(AC_5)_2$-sulfo-OSu dissolved in DMF was added to the aminated polyacrylamide beads dispersed in 100 mM borate buffer (pH 9.3) and the mixture was incubated for 1 h at 35°C. The molar amount of the added biotin derivative was about 1/20 of the molar contents of the amino groups. The biotinylated beads were precipitated with methanol and the precipitate was dispersed in 100 mM borate buffer (pH 9.3). The biotinylated beads were further reacted with an amino-reactive fluorophore, succinimidyl rhodamine green. The fluorophore dissolved in DMF was added to the biotinylated polyacrylamide beads and the mixture was incubated for 1 h at 50°C. The fluorescent biotinylated beads were precipitated with methanol and washed several times with methanol. The labeling procedure was repeated several times. The total molar amount of rhodamine green added was equal to the molar content of the free amino groups. The precipitate finally obtained was dispersed in water and dialyzed against water overnight. To block the residual free amino groups the fluorescent beads (5 mg/ml, 1 ml) were further reacted with acetic anhydride (97%, 50 μl) in 0.5 M NaH_2PO_4 (pH 7.0) for 15 min at room temperature, followed by precipitation with methanol, dispersion in water and dialysis against water. The resulting fluorescent biotinylated nanobeads contained about 10 biotin molecules and 20 to 30 rhodamine green molecules per one bead.

Characterization of Polyacrylamide Nanobeads—The particle size of the non-labeled polyacrylamide beads was estimated from quasi-elastic light scattering at various angles by the use of an instrument of our own manufacture. The translational diffusion coefficient was obtained from the correlation function and the diameter of the particles was calculated from the Einstein-Stokes equation. The particle size was about 35 nm in diameter. The fluorescent nanobeads attached to freshly cleaved mica were observed in buffer A with a scanning force microscope of our own manufacture. The height of the beads was around 30 nm. The molecular weight of the polyacrylamide nanobeads was determined by two methods (viscometry and particle counting). The intrinsic viscosity of non-labeled beads in 0.1 M NaCl aqueous solutions was measured with a Ubbelohde-type viscometer. To determine the molecular weight we used the following relationship, proposed by François *et al.* (*37*).

$$[\eta] = 9.33 \times 10^{-3}\ M_v^{0.75}\ \mathrm{cm^3/g}$$

Ten microliters of a diluted solution of fluorescent beads in 20 mM TES (pH 7.0) was put between two cover slips (22 $\times$ 22 mm) and left until all the beads became attached to the inner surfaces of the cover slips. Fluorescence images were taken at various sections of the cover slips. Then the number of particles within 50 $\times$ 50 μm areas was counted. From the average number and the dry weight, the molecular weight was estimated. The two methods gave a similar value, 10^6 Da.

Preparation of UltraAvidin-Coated Fluorescent Nanobeads—Since avidin and UltraAvidin tended to form clusters when their biotin sites were free, UltraAvidin (5 mg/ml, 0.3 ml) was mixed with HABA (1 mg/ml, 30 μl) in buffer C (10 mM imidazole-HCl, 10 mM KCl, 0.1 mM NaN_3, pH 7.6). The biotinylated fluorescent beads (6 mg/ml, 200 μl) were mixed with the HABA-UltraAvidin solution and the mixture was incubated overnight at 4°C. Since the beads contained 13.8 nmol of biotin and 5 mg of UltraAvidin contained 246 nmol of biotin sites, cross-linking of beads by UltraAvidin scarcely took place. UltraAvidin-coated beads were purified by the use of a gel filtration column (1.2 cm I.D. $\times$ 1 m, Bio-Gel A-0.5m,

Bio-Rad) equilibrated with buffer C.

Purification of HMM-Bead Complexes by Actin Affinity Chromatography—To purify HMM-bead complexes we developed actin affinity chromatography using myosin-extracted fibers. All procedures described here were carried out at 4°C. Two pieces of glycerinated rabbit psoas fibers, about 2 mm in diameter and 4 cm long, were chopped into short segments and homogenized in 30 ml of buffer R (30 mM KCl, 10 mM imidazole-HCl, 2 mM $MgCl_2$, 0.5 mM dithiothreitol, 1 mM EGTA, 20 μM PMSF, pH 7.6) by the use of a homogenizer (Ultra-Turrax T-25, IKA-Lab), for 30 to 60 s at 8,000 rpm. The fibers were collected by sedimentation at 3,300 × *g* for 10 min, then the pellet was dissolved in 5 ml of buffer R. The fiber suspensions were added to 3 ml of Bio-Gel (A-0.5m, Bio-Rad) swollen in buffer R. The mixture was gently mixed and allowed to settle into a column (1 cm in diameter). Polyacrylamide segments (about 1 mm in diameter) obtained by breaking a gel were used as bed supports. All washing steps mentioned below were done until protein was no longer detected in the eluates. Protein was monitored by measuring its fluorescence at 333 nm with excitation at 295 nm. All elutions were carried out at a constant flow rate of 0.4 ml/min. The column was washed first with buffer R plus 0.1% Triton X-100 and then with buffer R. To remove myosin from the fibers, 6 ml of an ATP-containing high-ionic solution (0.3 M KCl, 10 mM imidazole-HCl, 2 mM $MgCl_2$, 1 mM EGTA, 2 mM ATP, 0.5 mM dithiothreitol, 20 μM PMSF, pH 7.6) was applied to the column. Then the column was washed with the high-ionic solution without ATP, equilibrated with buffer R, washed again with buffer R plus 2 mM ATP, and finally equilibrated again with buffer R. Biotinylated HMM (1.6 μM, 13.8 μl) had been added to a 10-fold molar excess of UltraAvidin-coated fluorescent beads (108 nM, 2 ml) in buffer R and incubated overnight. The mixture was loaded on the affinity column. The eluate was collected and loaded on the column again. This loading-elution step was repeated eight times to ensure that all HMM-bead complexes were bound to actin in the fibers. The column was washed with buffer R until no fluorescent beads were detected in the eluate, monitoring the fluorescence at 545 nm with excitation at 505 nm. Finally HMM-beads were eluted with buffer R plus 2 mM ATP. About 28% of the HMM initially loaded on the column was recovered as HMM-bead complexes in the eluate. The purified HMM-beads were, however, greatly diluted during the purification processes (6.3 nM, 1 ml).

In Vitro Motility Assay—Motile activities of biotinylated HMM and bead-attached HMM were tested by observing actin filaments sliding on a glass cover slip coated with these HMM derivatives. As a control, the motile activity of intact HMM was also measured. For biotinylated HMM and intact HMM the assay was according to Toyoshima *et al.* (*23*), with a slight modification (cover slips for flow cells were treated with 0.2%, instead of 0.1%, nitrocellulose isopentyl acetate solution for 1 min). Actin filaments were labeled with tetramethylrhodamine-phalloidin. With bead-attached HMM the sample was not the one purified by actin affinity chromatography, since the concentration of the purified HMM-beads was too low for *in vitro* motility assay. Instead, bead-attached HMM was newly prepared in a flow cell as follows. First, cover slips for flow cells were cleaned as mentioned below and used without coating with nitrocellulose. UltraAvidin-coated beads, which had been labeled with rhodamine green to ensure good attachment to cover slips, were put into a flow cell and incubated for 10 min. The flow cell was washed with buffer F (25 mM KCl, 25 mM imidazole-HCl, 0.2 mM $CaCl_2$, 2 mM $MgCl_2$, 0.1 mM NaN_3, pH 7.6). Biotinylated HMM (1 μM in buffer F) was introduced into the flow cell. After 5 min, unattached biotinylated HMM was washed out with buffer F. Then, BSA (1 mg/ml in buffer F) was put into the cell, which was incubated for 2 min and was washed with buffer F. Sliding of actin filaments was observed under an epifluorescence microscope (Olympus IX70; equipped with an oil-immersion objective, 100×, NA 1.35), the images being taken with an SIT camera (C2741-08, Hamamatsu Photonics).

Fluorescence Visualization of Individual HMM Molecules—Actin filaments labeled with tetramethylrhodamine phalloidin were observed with the G-filter set, while fluorescent polyacrylamide beads labeled with rhodamine green were observed with the B-filter set. The HMM-bead complexes used here were those purified by actin affinity chromatography as mentioned above. The rigor complexes were prepared by mixing the HMM-beads (0.1 nM, 0.5 ml) with tetramethylrhodamine phalloidin-labeled actin filaments (2.5 μM, 5.0 μl) and apyrase (1 mg/ml, 25 μl). They were allowed to stand at 25°C for 1 h. After the addition of 1% 2-mercaptoethanol the sample was applied to a flow cell made from freshly cleaned cover slips (without any coating) and incubated for 5 min. The fluorescence images of the rigor complexes were observed, then the cells were washed with buffer R plus 2 mM ATP and the fluorescence images were observed again. The fluorescence microscope and the video camera used here were the same as above.

Imaging by an Atomic Force Microscope—The atomic force microscope (AFM) combined with an epifluorescence microscope (IMT2, Olympus) was of our own manufacture. A solution of HMM-beads that had been purified by actin-affinity column chromatography was put on a freshly cleaved mica surface, left for 30 min, and then washed with buffer F. The AFM images were taken in buffer F in constant-force mode (10 pN), using a micro cantilever with a spring constant of 20 pN/nm (OMCL-TR400PS-2, Olympus).

Other Assays—SDS-PAGE was performed in a 7.0-15.0% polyacrylamide gradient containing 0.1% SDS (*39*).

The ATPase activities of acto-HMM (0.1 mg/ml HMM or biotinylated HMM and various concentrations of actin) were assayed in 10 mM Tris-HCl (pH 7.9), 2.5 mM $MgCl_2$, and 2.5 mM ATP at 25°C.

Cleaning of Glass Cover Slips—Glass cover slips were bath-sonicated in 3% cleaning detergent for 30 min, rinsed with water exhaustively and boiled in water for 5 min. Then they were incubated in an 8 : 1 (v/v) mixture of sulfuric acid and hydrogen peroxide at 80°C for 15 min, rinsed with water, boiled twice in water for 5 min each, and dried at 40°C.

RESULTS

Enzymatic Labeling of HMM—HMM was incubated with guinea-pig transglutaminase in the presence of dansylcadaverine and then purified by gel chromatography. The HMM sample showed green fluorescence characteristic of the dansyl group. In order to know whether the labeling had

taken place covalently the HMM was run on SDS gels. A fluorescent band appeared on the heavy chains, but not on the light chains (lanes a and c in Fig. 1). In order to determine labeled regions within the heavy chains, the HMM was cleaved with chymotrypsin and run on SDS gels With the digests of an HMM sample that had been incubated with transglutaminase for 3 h the 60K segment corresponding to S-2 was predominantly fluorescent (lane e). With the HMM sample of 5 h incubation a weakly fluorescent band additionally appeared on the 98K segment that corresponded to S-1 heavy chains (lane g). These observations revealed that transglutaminase-mediated labeling took place primarily in the S-2 region of HMM.

Time Course of Incorporation of Cadaverine Derivatives into HMM—We first determined fluorometrically how many moles of dansylcadaverine were attached to HMM. Since the fluorescence of the dansyl group is quite sensitive to its environment, the samples of dansyl-labeled HMM were pretreated by exhaustive digestion with chymotrypsin. Their fluorescence intensities were compared with that of a known concentration of dansylcadaverine. The emission spectrum of free dansylcadaverine peaked around 542 nm, whereas that of dansylcadaverine conjugated to HMM peaked around 500 nm. Upon chymotryptic digestion of the labeled HMM the blue-shifted peak returned to 542 nm. As shown by closed triangles in Fig. 2, the number of dansylcadaverine moieties incorporated initially increased with increasing incubation time and was nearly saturated after 3 to 4 h. The saturation level appeared to be 4 mol of dansylcadaverine per 1 mol of HMM. In consequence, each heavy chain has two sites for the labeling in the S-2 region. For the purpose of attaching a fluorescent nanosphere to HMM, the strong affinity between biotin and avidin is quite useful. Therefore we also examined the time-course of transglutaminase-catalyzed incorporation of biotin using biotincadaverine. It is natural to expect that, like dansylcadaverine, biotincadaverine will also be incorporated primarily into the S-2 region of HMM. As shown in Fig. 2

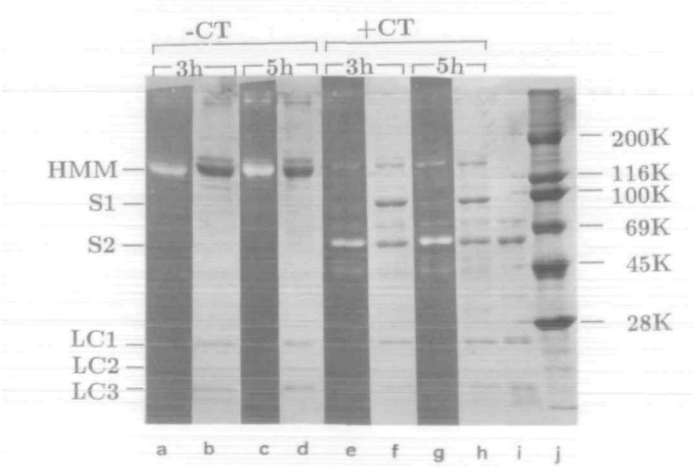

Fig 1. **Locations within HMM of dansylcadaverine incorporated by the transglutaminase reaction.** The reaction was allowed to continue for 3 h (lanes a, b, e, f) or 5 h (lanes c, d, g, h). The samples were digested with chymotrypsin after dansylcadaverine incorporation (lanes e, f, g, h) The gels were exposed to UV to see the fluorescence due to dansylcadaverine (lanes a, c, e, g), and then stained with Coomassie Blue (lanes b, d, f, h). Lane i, partially purified S-2; lane j, size markers

biotincadaverine was attached to HMM, the amount initially increasing with time and then becoming saturated. As indicated by the example in Fig. 3, the quantity of biotin incorporated was estimated using the competitive binding of HABA to avidin and the concomitant increase in the absorbance at 510 nm. HABA does not bind to avidin until the concentration of biotin sites of avidin exceeds the concentration of biotin, since the affinity of biotin is much higher than that of HABA. Thereafter, the absorbance at 510 nm increases with increasing avidin concentration. As shown by closed squares in Fig. 2 the number of moles of

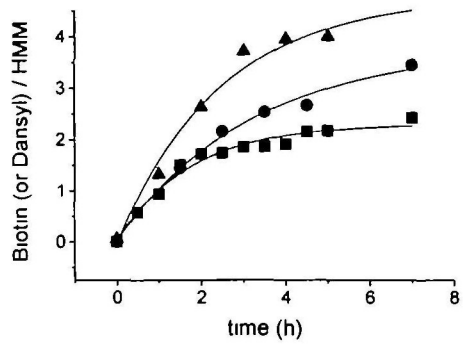

Fig 2 **Time-course of incorporation of dansylcadaverine and biotincadaverine into HMM.** The amounts of dansylcadaverine (▲) were estimated from the fluorescence intensity at 550 nm with excitation at 330 nm. Because the fluorescence intensity of the dansyl moiety was environment-sensitive, the labeled-HMM was digested exhaustively with chymotrypsin The quantities of biotincadaverine (●, ■) were estimated as described in "MATERIALS AND METHODS" (also see Fig. 3). In the first assay the biotin-labeled HMM was not digested (■), but in the second assay it was digested exhaustively with chymotrypsin (●). The digestion was terminated by adding PMSF.

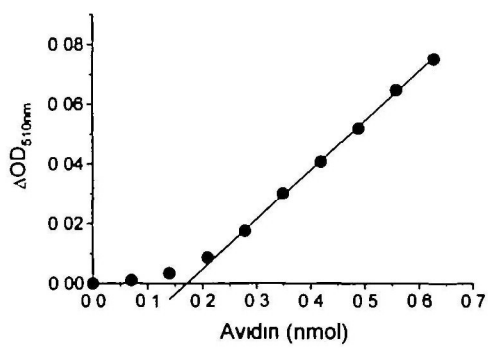

Fig. 3. **Colorimetric determination of biotin.** HABA (4 mM, 20 μl) was added to biotinylated HMM (0 64 μM, 0 5 ml) that had been prepared by incubation for 4.5 h in the presence of biotincadaverine and transglutaminase Then 5 μl of an avidin solution (1 mg/ml) was added several times to the mixture in a stepwise manner Ten minutes after each addition the optical density at 510 nm was read. The base value (without avidin) was subtracted. When the amount of avidin was small, ΔOD stayed at a low level. When the amount of avidin was further increased, ΔOD linearly increased with increasing avidin concentration. The biotin content was estimated from the intercept given by extrapolation of the linear plot of ΔOD *vs* amount of avidin to the abscissa. The biotin content was given by 4 times the amount of avidin at the intercept. In the present case it was $4\times0.17=0.68$ nmol The amount of HMM was $0.64\times0.5=0.32$ nmol. These values gave a molar ratio of 2.1 biotins/HMM.

biotin detected per 1 mol of HMM seemed to reach saturation at two. Since avidin is relatively large and its biotin sites are not on the surface, but are located in deep clefts (*38*), not all the biotins bound to HMM may be accessible to avidin. Therefore, the biotin-labeled HMM was exhaustively digested with chymotrypsin and assayed again. With the HMM samples that had been incubated for less than 90 min with transglutaminase the chymotryptic digestion revealed no additional biotin. However, with the HMM samples that had been incubated longer than 90 min the digestion revealed additional biotin. Therefore the two biotins that reacted relatively quickly were exposed, but additional biotins were not exposed in the non-digested HMM.

Actin-Activated ATPase—We examined the effect of biotin incorporation into HMM upon the actin-activated ATPase activity of HMM. The actin concentration was varied to estimate the maximum ATPase activity (V_m). As shown by black bars in Fig. 4, V_m was moderately decreased with increasing incubation time. Since HMM was incubated at 25°C for a long time, the transglutaminase reaction might not be solely responsible for the moderate deactivation of HMM. As a control, therefore, we examined how incubation of HMM at 25°C without transglutaminase would affect the ATPase activity. As shown by white bars in Fig. 4 the transglutaminase-absent incubation also moderately deactivated the actin-activated ATPase to almost the same extent as did the transglutaminase-present incubation. Therefore, we concluded that biotin incorporation into HMM did not affect the actin-activated ATPase activity.

Motile Activity of Biotinylated HMM—Biotin was very likely incorporated primarily into the S-2 region of HMM; moreover, the biotin incorporation did not affect the actin-activated ATPase activity. We consequently expected that the biotin incorporation would not affect the ability of HMM to glide actin filaments. We confirmed this expectation as follows. As shown in Table I, actin filaments slid on biotin-labeled HMM at a velocity of 4.7 μm/s on average. This velocity is similar to that observed with non-labeled HMM. Here, the biotin-labeled as well as non-labeled HMM had been allowed to stand for 3 h at 25°C in the presence and absence of transglutaminase, respectively. We further examined the effect of UltraAvidin-bead binding to biotinylated HMM upon the motile activity of HMM. For this examination cover slips of a flow cell were first coated with UltraAvidin-bound polyacrylamide beads, followed by coating with HMM and then with BSA. When biotinylated HMM was used in the HMM-coating actin filaments slid on the surface at a velocity of 4.5 μm/s. To confirm that biotinylated HMM had been attached to the surface through the specific binding between biotin and UltraAvidin, not through non-specific binding of HMM to the UltraAvidin-bound polyacrylamide or to the cover slip itself, non-labeled HMM was used as the coating. In this control, actin filaments never became attached to the surface, implying that non-labeled HMM was not able to bind to the surface coated with UltraAvidin-bound polyacrylamide beads. Thus, attachment through specific binding was confirmed. Consequently we concluded that binding of either UltraAvidin or UltraAvidin-bead to biotinylated HMM did not affect the motile activity of HMM. This also strongly suggested that biotin had been incorporated primarily into the S-2 region, otherwise binding of a relatively sizable UltraAvidin-bead to HMM would have affected the motile activity of HMM.

Visualization of HMM-Beads—As mentioned in "MATERIALS AND METHODS," HMM-beads were purified by actin affinity chromatography. The HMM-beads thus purified therefore had been bound to actin in the fibers and had been dissociated from actin by the addition of ATP. We confirmed that the HMM-beads thus purified had the native properties of intact HMM. The solution of purified HMM-beads contained ATP. To form rigor complexes the HMM-bead and actin filaments were therefore mixed in the presence of apyrase. To ensure visualization of individual HMM-beads on actin a large molar excess of actin was used (25 nM actin, 0.1 nM HMM-beads). The solution was put into a flow cell made from cleaned cover slips, and left for 10 min. The flow cell was then washed by flowing a buffer solution through it. The sample was observed under a fluorescence microscope with two different optical filter sets, one being for tetramethylrhodamine (actin) and the other for rhodamine green (HMM-beads). As shown in Fig. 5b, HMM-beads were clearly seen, being found in the places where actin filaments were located (Fig. 5a). The brightness of the HMM-beads on actin was similar to that of beads alone (shown in the larger photograph). Therefore, the images of HMM-beads on actin were considered to be those of individual HMM-bead complexes. After the flow cell was washed with a buffer solution containing 2 mM ATP, actin filaments disappeared (Fig. 5c), while the HMM-beads remained attached to the same places as before washing (Fig. 5d). From these observations, together with the intact motility of HMM bound to Ultra-

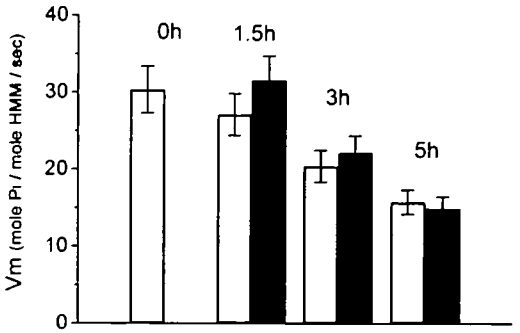

Fig. 4. **Effect of biotincadaverine incorporation upon the actin-activated ATPase activity of HMM.** The ATPase activities at 25°C were measured immediately after the transglutaminase reaction was terminated by the addition of EGTA. Values of V_m of the actin-activated ATPase were estimated from Lineweaver-Burk plots of the ATPase activity *vs.* actin concentration. Black bars, biotin-labeled HMM; white bars, control HMM incubated without transglutaminase.

TABLE I. **Sliding velocity of actin filaments on HMM and HMM-bead complexes.** Data in the table are mean velocities ± SD for the number of observation indicated in parentheses.

	Nitrocellulose-coated cover slip (μm/s)	UltraAvidin-bead-coated cover slip (μm/s)
Control[a]	4.8 ± 1.0 (n = 34)	—[c]
Biotinylated HMM[b]	4.7 ± 0.9 (n = 34)	4.5 ± 0.8 (n = 35)

[a]HMM incubated for 3 h without transglutaminase. [b]HMM incubated for 3 h in the presence of transglutaminase and biotincadaverine. [c]No actin filaments were found on the surface, due very likely to the absence of attached HMM.

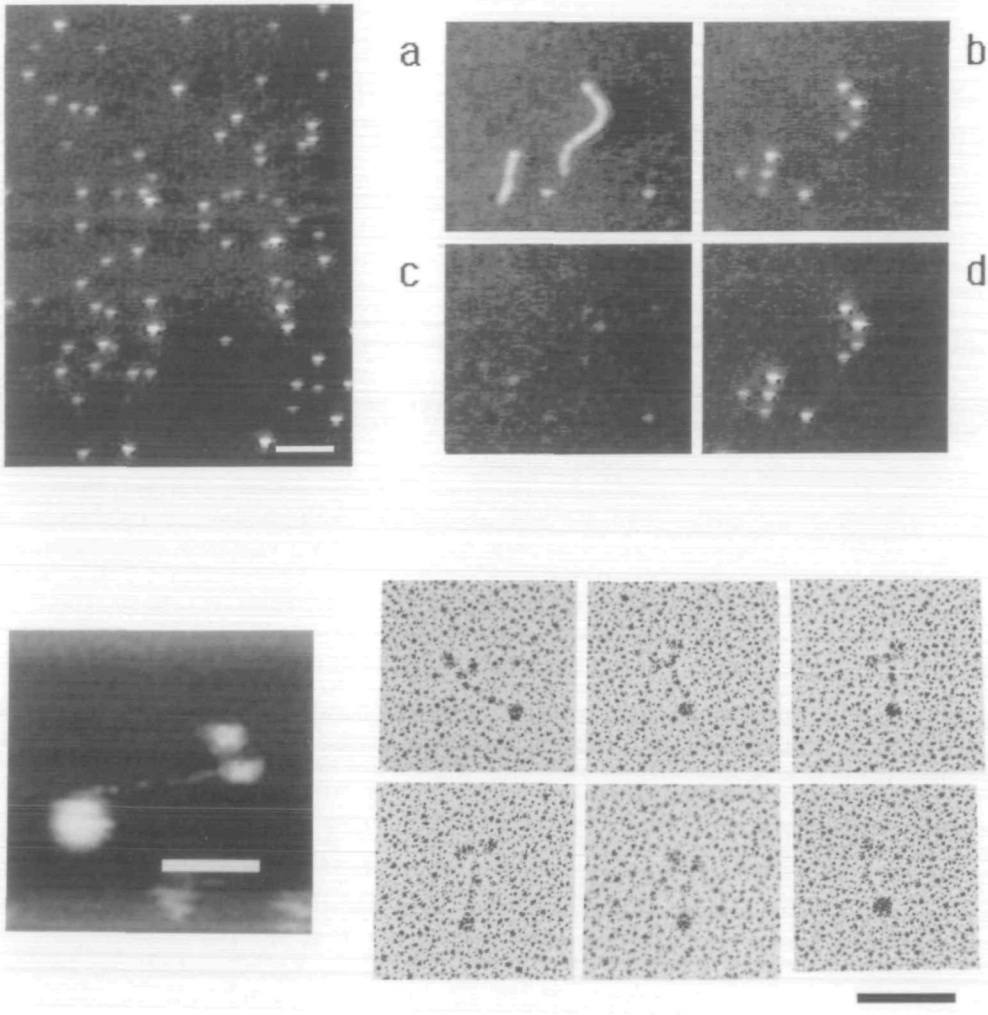

Fig. 5 **Fluorescence images of beads alone, actin-HMM-bead complexes, and HMM-beads attached to a glass cover slip.** The images were obtained using a G-filter set (a, c) for the observation of tetramethylrhodamine phalloidin-labeled actin filaments and a B-filter set (the large picture, b, d) for the observation of rhodamine-green-labeled beads, before (a, b) and after (c, d) washing with a buffer solution containing 2 mM ATP. Actin filaments were swept out by the washing, whereas HMM-beads remained. The sample of acto-HMM-bead complexes had been obtained by mixing 0.1 n HMM-beads and 25 nM actin. Scale bars, 6 μm.M

Fig. 6 **An AFM image and a gallery of electron microscopic images of bead-HMM conjugates.** An AFM image of an HMM-bead conjugate on a mica surface was taken in buffer F (left-hand side). Scale bar, 50 nm. EM images of bead-HMM conjugates are shown on the right-hand side. The sample in 50% glycerol was sprayed onto a mica surface and then the particles on the mica were rotary-shadowed with Pt-C vapor granules at an angle of 10°. Scale bar, 100 nm. The bead-HMM preparation was the same as that used in Fig. 5.

Avidin-beads, it was clear that the HMM-bead complex retained the characteristics of intact HMM.

AFM and Electron Microscopic Observations of Bead-Attached HMM—The biochemical analyses mentioned above allowed us to identify the biotinylation sites within HMM as almost certainly on the S-2 region of HMM. To confirm this and further to establish the location within S-2, an HMM sample that had been labeled with UltraAvidin-coated polyacrylamide nanobeads was observed by AFM and by electron microscopy. In the AFM images we saw a spherical particle positioned near a two-headed structure. In between them a misty, string-like structure was sometimes observed (Fig. 6, left-hand image). Because the image of the string-like structure was unclear, we could not reach a definite conclusion as to the location of nanobeads within the labeled HMM. Dr. Katayama of the University of Tokyo kindly took electron micrographs of an HMM sample that had been rotary-shadowed on a mica surface. As can be seen in Fig. 6, the beads are positioned in the distal end of S-2 (near the S-2/LMM junction). The dimensions of nanobeads in the electron micrographs were somewhat smaller than those we expected from the dimensions of UltraAvidin and of polyacrylamide nanobeads in an aqueous solution.

DISCUSSION

The purpose of the present study was to develop a method by which HMM could be attached to a fluorescent nanosphere without losing its motile activity. Recently Funatsu *et al.* (*40*) have succeeded in visualizing single fluorescent molecules in aqueous solution using an improved fluorescence microscope and a highly sensitive video camera. They have imaged individual molecules of myosin and a myosin-bound ATP analogue that are labeled with single fluorophores. Their study was an important step towards developing a unimolecular physiology of motor proteins, through localizing individual molecules of interest by imaging them with a fluorescence video-microscope. A possible application might be as follows. Using an atomic force microscope we may be able to measure the force generated by a single HMM molecule that is fixed to the apex of a cantilever tip and is interacting with an actin filament fixed onto a flat substratum. With blind scanning of a cantilever (or the sample stage) it is difficult to capture a single HMM molecule at the apex, whereas pinpointing individual HMMs would facilitate moving the apex of the cantilever tip to a single HMM molecule. It is not necessarily important to limit the number of fluorophores to be attached to

unity, as long as the labeling does not cause any deactivation of the protein. As long as no deactivation takes place, incorporation of a large number of fluorophores is advantageous. The reason is that intense illumination of the fluorophore leads to photobleaching; in consequence, the survival time of single fluorophores under intense illumination is rather short. In the case of Funatsu *et al.* the survival time was 85 s under their experimental conditions. The larger the number of fluorophores incorporated, the longer the survival time; in other words, a longer observation time is attained. In our case there was practically no limitation to the observation time.

It has been shown here that dansylcadaverine was conjugated enzymatically to HMM predominantly at the S-2 region, with a very minor labeling at the heavy chains of the S-1 region. The light chains were never labeled. The glutamine residue to be attacked by transglutaminase should be in a flexible region of the protein (*41*), since the γ-carboxamide group of glutamine has to be captured transiently in the active site of transglutaminase for the formation of a transient γ-glutamyl thioester with concomitant release of ammonia (the thiol group is that of the active site cysteine). Actin, for instance, is enzymatically labeled at Gln-41 (*26*), which resides on a flexible loop spanning between Pro-38 and Ser-52 (*42*). In the case of His-388→Gln-388 mutant of yeast phosphoglycerate kinase, the site modified by transglutaminase is Gln-388 in the hinge region of the mutant kinase (*43*). It is known that regions at the S-1/S-2 junction and at the S-2/LMM junction have flexible structures. The N-terminal region of S-2 does not contain glutamine residues, while the C-terminal region of S-2 does contain glutamine [Gln-417, Gln-426; the sequence is numbered starting at the N-terminal of S-2 (*44, 45*); the C-terminal end of S-2 is Phe-437 (*46*)]. Therefore, these glutamine residues are the most likely candidates for labeling targets.

Using activated human plasma fibrinoligase, which is also called blood coagulation factor XIII and can have transglutaminase activity, Cohen *et al.* labeled rabbit skeletal myosin with dansylcadaverine (*47*). They observed that dansylcadaverine was incorporated into both heavy and light chains of myosin, and that the incorporation into the light chains was less than that into the heavy chains. As far as the susceptibility of the light chains to the transferase action is concerned, the difference between our result and theirs seems to be due to the difference in specificity between the two types of transglutaminases. We have examined another type of transglutaminase that originated from fish meat, but has been mass-produced by gene engineering. The enzyme does not require calcium for its activity. The enzyme was a gift from Ajinomoto Foods and was purified by DEAE ionic exchange chromatography. The fish transglutaminase conjugated dansylcadaverine to HMM at both the S-1 and S-2 regions of the heavy chains equally, greatly reducing the motile activity of HMM (unpublished result). So, different types of transglutaminases have different specificity as to the target sites within the same protein substrate.

We did not establish biochemically where within HMM biotincadaverine was attached. However, it is reasonable to infer that both dansylcadaverine and biotincadaverine were conjugated to the same glutamine residues, since the sites targeted by guinea-pig transglutaminase are common irrespective of the amino substrate. The electron micrographs of biotinylated HMM attached to UltraAvidin-coated polyacrylamide nanobeads clearly showed the bound beads positioned at the distal end of S-2 (near the S-2/LMM junction). Therefore, the bead was presumably bound to biotin that had been conjugated at either Gln-417 or Gln-426. The number of biotins incorporated into an HMM molecule was not established. Even the exhaustive digestion of the biotinylated HMM revealed only a small additional quantity of biotin. Although there is ambiguity as to this point, it is clear that an HMM molecule can have at most two biotins on S-2 that are accessible to avidin. Before the present study, several sites within HMM were known to be available for chemical labeling. Among them only sites on LC2 are available for innocuous labeling with small molecules. However, we do not know yet whether LC2 labeling with large molecules such as nanospheres (or the apex of a cantilever tip, although it is not a molecule) are still innocuous. Sizable molecules linked to HMM at LC2 may touch HMM at side chains that play a key role in the HMM's motile function and may eventually deactivate HMM. The method for innocuous labeling presented here should be valuable for studies on the unimolecular physiology of the actomyosin motor.

We would like to thank Dr. Eisaku Katayama of the University of Tokyo for taking electron micrographs of the HMM-bead sample, and Prof. Kijiro Kon-no of Tokyo Science University for valuable advice on the preparation of polyacrylamide nanospheres.

REFERENCES

1. Sheetz, T. and Spudich, J.A. (1983) Movement of myosin-coated fluorescent beads on actin cables *in vitro*. *Nature* **303**, 31-35
2. Shimmen, T. and Yano, M. (1984) Active sliding movement of latex beads coated with skeletal muscle myosin on Chara actin bundles. *Protoplasma* **121**, 132-137
3. Yanagida, T., Nakase, M., Nishiyama, K., and Oosawa, F. (1984) Direct observation of motion of single F-actin filaments in the presence of myosin. *Nature* **307**, 58-60
4. Kron, S.J. and Spudich, J.A. (1986) Fluorescent actin filaments move on myosin fixed to a glass surface. *Proc. Natl. Acad. Sci. USA* **83**, 6272-6276
5. Kishino, A. and Yanagida, T. (1988) Force measurements by micromanipulation of a single actin filament by glass needles. *Nature* **334**, 74-76
6. Ashkin, A. and Dziedzic, J.M. (1987) Optical trapping and manipulation of viruses and bacteria. *Science* **235**, 1517-1520
7. Ashkin, A., Schütze, K., Dziedzic, J.M., Euteneuer, U., and Schliwa, M. (1990) Force generation of organelle transport measured in vivo by an infrared laser trap. *Nature* **348**, 346-348
8. Block, S.M., Goldstein, L.S.B., and Schnapp, B.J. (1990) Bead movement by single kinesin molecules studied with optical tweezers. *Nature* **348**, 348-352
9. Saito, K., Aoki, T., Aoki, T., and Yanagida, T. (1994) Movement of single myosin filaments and myosin step size on an actin filament suspended in solution by a laser trap. *Biophys. J.* **66**, 769-777
10. Finer, J.T., Simmons, R.M., and Spudich, J.A. (1994) Piconewton forces and nanometre steps. *Nature* **368**, 113-119
11. Lal, R. and John, S.A. (1994) Biological applications of atomic force microscopy. *Am. J. Physiol.* **266**, c1-c21
12. Hansma, H.G. and Hoh, J.H. (1994) Biomolecular imaging with the atomic force microscope. *Annu. Rev. Biophys. Biomol. Struct.* **23**, 115-139
13. Sekine, T. and Yamaguchi, M. (1963) Effect of ATP on the binding of *N*-ethylmaleimide to SH groups in the active site of myosin ATPase. *J. Biochem.* **54**, 196-198

14. Sekine, T., Barnett, L., and Kielley, W.W. (1962) The active site of myosin adenosine triphosphatase. *J. Biol. Chem.* **237**, 2769-2772
15. Kubo, S., Tokura, S., and Tonomura, Y. (1960) On the active site of myosin A-adenosine triphosphatase. I. Reaction of the enzyme with trinitrobenzenesulfonate. *J. Biol. Chem.* **235**, 2835-2839
16. Okamoto, Y. and Yagi, K. (1976) Ca^{2+}-induced conformational changes of spin-labeled g_2 chain bound to myosin and the effect of phosphorylation. *J. Biochem.* **80**, 111-120
17. Bagshaw, C.R. and Kendrick-Jones, J. (1980) Identification of the divalent metal ion binding domain of myosin regulatory light chains using spin-labelling techniques. *J. Mol. Biol.* **140**, 411-433
18. Arata, T. (1990) Orientation of spin-labeled light chain 2 of myosin heads in muscle fibers. *J. Mol. Biol.* **214**, 471-478
19. Kielley, W.W. and Bradley, L.B. (1956) The relationship between sulfhydryl groups and the activation of myosin adenosinetriphosphatase. *J. Biol. Chem.* **218**, 653-659
20. Chaen, S., Muraoka, A., and Sugi, H. (1991) Effect of partial inactivation of myosin heads on the ATP-dependent actin-myosin sliding. *Biophys. J.* **59**, 430a
21. Moss, R.L., Guilian, G.G., and Greaser, M.L. (1982) Physiological effects accompanying the removal of myosin LC_2 from skinned skeletal muscle fibers. *J. Biol. Chem.* **257**, 8588-8591
22. Yamamoto, K. and Sekine, T. (1977) Fluorometric studies on the light chains of skeletal muscle myosin. *J. Biochem.* **82**, 747-752
23. Toyoshima, Y.Y., Kron, S.J., McNally, E.M., Niebling, K.R., Toyoshima, C., and Spudich, J.A. (1987) Myosin subfragment-1 is sufficient to move actin filaments in vitro. *Nature* **328**, 536-539
24. Folk, J.E. (1983) Mechanism and basis for specificity of transglutaminase-catalyzed ε-(γ-glutamyl) lysine bond formation. *Adv. Enzymol.* **54**, 1-56
25. Takashi, R. and Kasprzak, A.A. (1985) New fluorescent labels in skeletal muscle actin and acto-S-1 distances. *Biophys. J.* **47**, 26a
26. Takashi, R. (1988) A novel actin label: A fluorescent probe at glutamine-41 and its consequences. *Biochemistry* **27**, 938-943
27. Giordano, M., Takashi, R., and Ando, T. (1986) A new fluorescent label for skeletal muscle HMM which does't alter its ATPase activity. *Biophys. J.* **49**, 444a
28. Ando, T., Yamamoto, T., Kobayashi, N., and Munekata, E. (1992) Synthesis of a highly luminescent terbium chelate and its application to actin. *Biochim. Biophys. Acta* **1102**, 186-194
29. Tonomura, Y., Appel, P., and Morales, M.F. (1966) On the molecular weight of myosin. *Biochemistry* **5**, 515-521
30. Weeds, A.G. and Pope, B. (1977) Studies on the chymotryptic digestion of myosin. Effect of divalent cations on proteolytic susceptibility. *J. Mol. Biol.* **111**, 129-157
31. Ando, T. and Asai, H. (1979) Conformational change in actin filament induced by the interaction with heavy meromyosin: Effects of pH, tropomyosin and deoxy-ATP. *J. Mol. Biol.* **129**, 265-277
32. Spudich, J.A. and Watt, S. (1971) The regulation of rabbit skeletal muscle contraction. I. Biochemical studies of the tropomyosin-troponin complex with actin and the proteolytic fragments of myosin. *J. Biol. Chem.* **246**, 4866-4871
33. Lowry, O.H., Rosebrough, N.J., Farr, A.L., and Randall, R.J. (1951) Protein measurement with the folin phenol reagent. *J. Biol. Chem.* **193**, 265-275
34. Green, N.M. (1965) A spectrophotometric assay for avidin and biotin based on binding of dyes by avidin. *Biochem. J.* **94**, 23c-24c
35. Candau, F. and Leong, Y.S. (1985) Kinetic study of the polymerization of acrylamide in inverse microemulsion. *J. Polymer Sci.* **23**, 193-214
36. Kitahara, A. and Kon-no, K. (1966) Mechanism of solubilization of water in nonpolar solutions of oil-soluble surfactants: Effect of electrolytes. *J. Phys. Chem.* **70**, 3394-3398
37. François, J., Sarazin, D., Schwarts, T., and Weill, G. (1979) Polyacrylamide in water: Molecular weight dependence of $\langle R^2 \rangle$ and $[\eta]$ and the problem of the excluded volume exponent. *Polymer* **20**, 969-975
38. Pugliese, L., Coda, A., Malcovati, M., and Bolognesi, M. (1993) Three-dimensional structure of the tetragonal crystal form of egg-white avidin in its functional complex with biotin at 2 Å resolution. *J. Mol. Biol.* **231**, 698-710
39. Laemmli, U.K. (1970) Cleavage of structural proteins during the assembly of the head of bacteriophage T4. *Nature* **277**, 680-685
40. Funatsu, T., Harada, Y., Tokunaga, M., Saito, K., and Yanagida, T. (1995) Imaging of single fluorescent molecules and individual ATP turnovers by single myosin molecules in aqueous solution. *Nature* **374**, 555-559
41. Berbers, G.A.M., Bentlage, H.C.M., Brans, A.M.M., Bloemendal, H., and de Jong, W.W. (1983) β-Crystallin: Endogenous substrate of lens transglutaminase characterization of the acyl-donor site in the β B_p chain. *Eur. J. Biochem.* **135**, 315-320
42. Kabsch, W., Mannherz, H.G., Suck, D., Pai, E.F., and Holmes, K.C. (1990) Atomic structure of the actin: DNase I complex. *Nature* **347**, 37-44
43. Coussons, P.J., Kelly, S.M., Price, N.C., Johnson, C.M., Smith, B., and Sawyer, L. (1991) Selective modification by transglutaminase of a glutamine side chain in the hinge region of the histidine-388→glutamine mutant of yeast phosphoglycerate kinase. *Biochem. J.* **273**, 73-78
44. Capony, J.-P. and Elzinga, M. (1981) The amino acid sequence of a 34,000 dalton fragment from S-2 of myosin. *Biophys. J.* **33**, 148a
45. Maeda, K., Sczakiel, G., and Wittinghofer, A. (1987) Characterization of cDNA coding for the complete light meromyosin portion of a rabbit fast skeletal muscle myosin heavy chain. *Eur. J. Biochem.* **167**, 97-102
46. Maita, T., Yajima, E., Nagata, S., Miyanishi, T., Nakayama, S., and Matsuda, G. (1991) The primary structure of skeletal muscle myosin heavy chain: IV. Sequence of the rod, and the complete 1,938-residue sequence of the heavy chain. *J. Biochem.* **110**, 75-87
47. Cohen, I., Young-Bandala, L., Blankenberg, T.A., Siefring, G.E., Jr., and Bruner-Lorand, J. (1979) Fibrinoligase-catalyzed cross-linking of myosin from platelet and skeletal muscle. *Arch. Biochem. Biophys.* **192**, 100-111